Supplemental Information

Coordination of receptor tyrosine kinase signaling and interfacial tension dynamics drive radial intercalation and tube elongation

Neil M. Neumann, Matthew C. Perrone, Jim H. Veldhuis, Robert J. Huebner, Huiwang Zhan, Peter N. Devreotes, G. Wayne Brodland, and Andrew J. Ewald

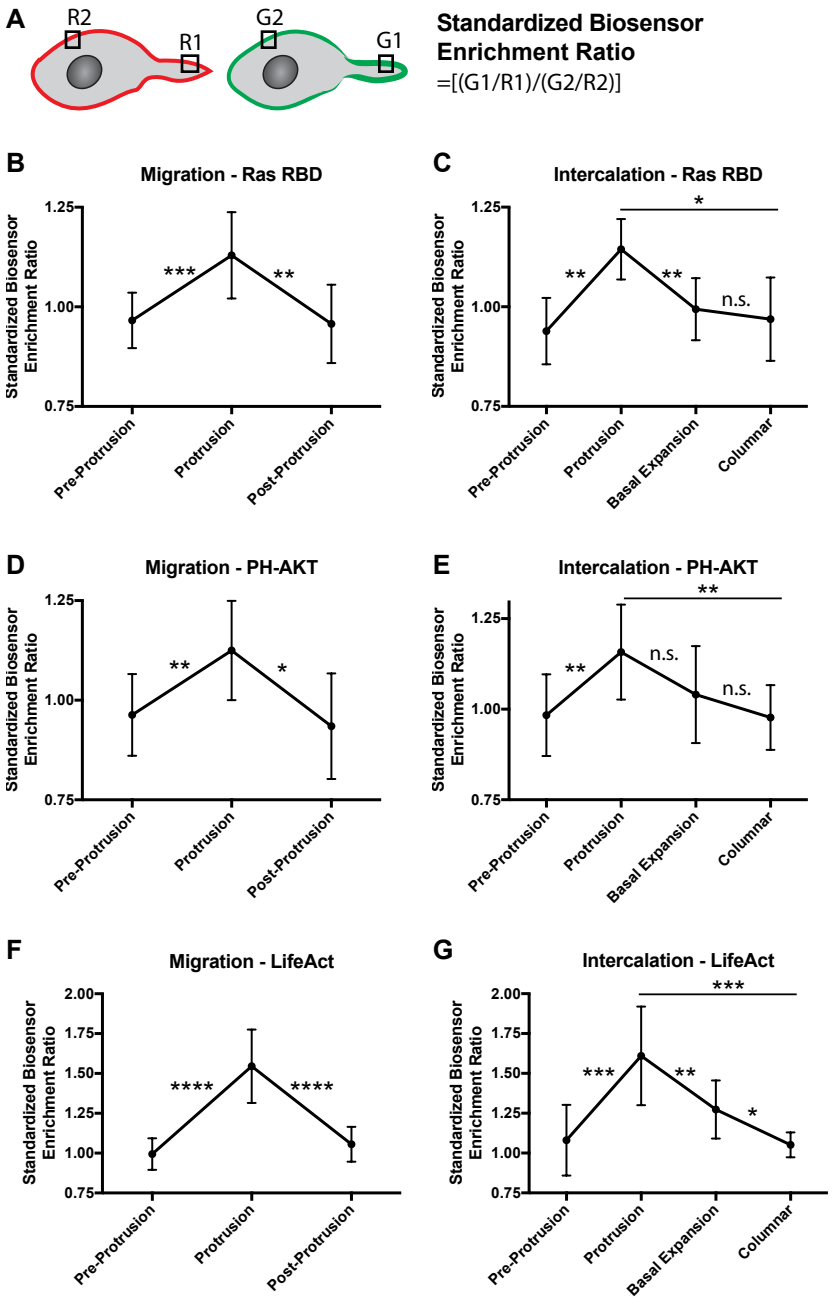

Figure S1 (Related to Figure 1 and 5) Quantification of fluorescent biosensor enrichment in protrusions during migration and radial intercalation.

(A) Schematic used to determine the standardized biosensor enrichment ratio: [(G1/R1)/(G2/R2)]. A 4 μm2 region of interest was used to quantify enrichment of biosensor (green) over membrane marker (tdTomato, red) compared to a reference region of interest. **(B,D,F)** Quantification of biosensor enrichment during cell migration within the stratified epithelium. Protrusions enriching biosensor were visually identified, followed by pre- and post-protrusions. **(C,E,G)** Quantification of biosensor enrichment during radial intercalation. Protrusions enriching biosensor were visually identified, followed by pre-protrusion, basal expansion, and columnar. **(B)** Ras activity (Raf1(RBD)-GFP, green) during migration. 9 orgs, r=3. **(C)** Ras activity (Raf1(RBD)-GFP, green) during radial intercalation. 10 orgs, r=3. **(D)** PIP3 biosensor (PH-Akt-GFP, green) during migration. 9 orgs, r=3. **(E)** PIP3 biosensor (PH-Akt-GFP, green) during radial intercalation. 8 orgs, r=2. **(F)** F-actin biosensor (LifeAct-GFP, green) during migration.10 orgs, r=3. **(G)** F-actin biosensor (LifeAct-GFP, green) during radial intercalation. 11 cells, 10 orgs, r=4. N=10 cells for each condition, unless otherwise stated. Statistics test performed include: repeated measures one-way ANOVA with the Greenhouse-Geisser correction and Tukey's multiple comparisons test with individual variances computed for each comparison. n.s. $p > 0.05$, *$p<0.05$, **$p<0.01$, ***$p<0.001$, ****$p<0.0001$.

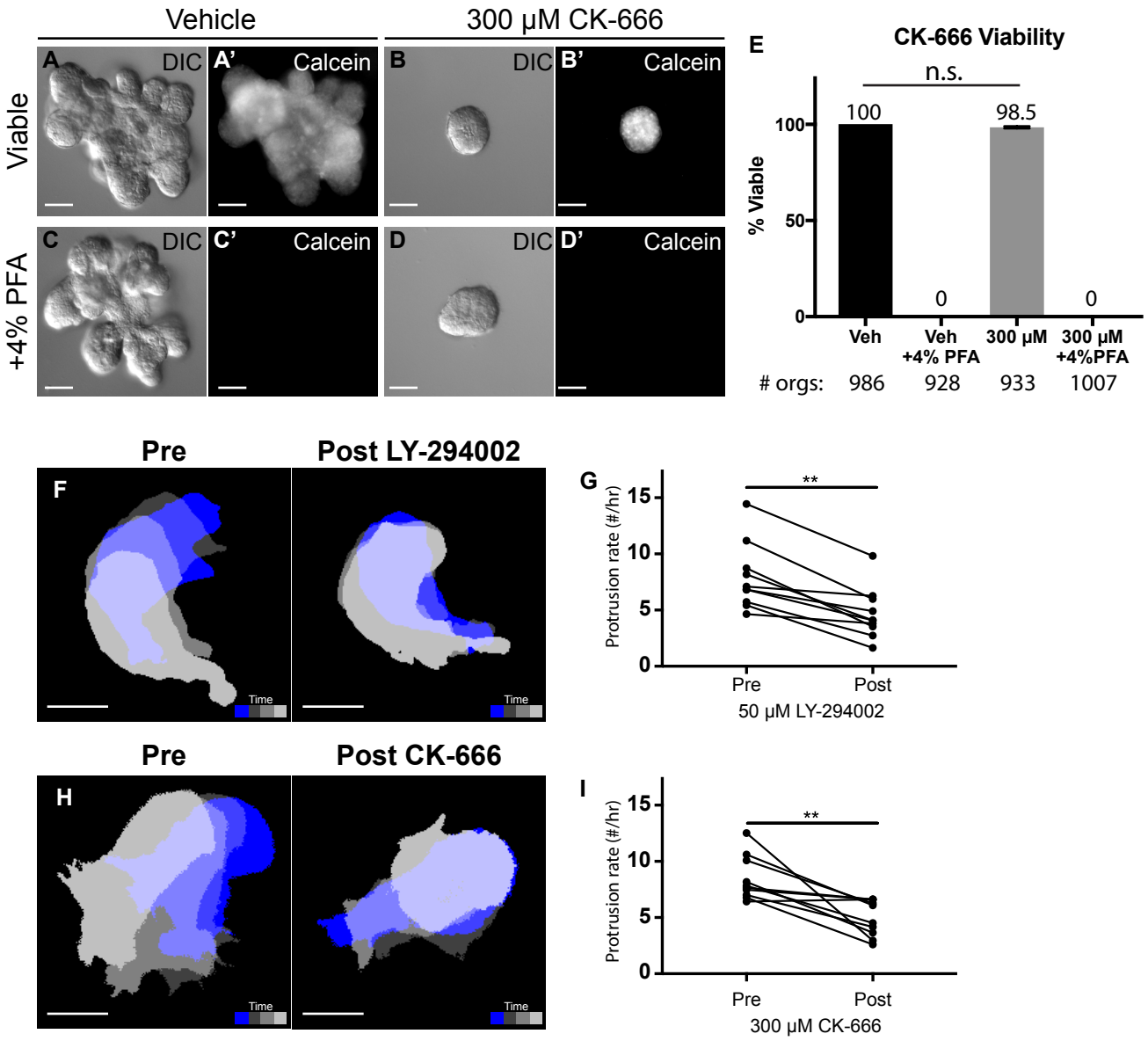

Figure S2 (Related to Figure 2) Arp2/3 inhibitor-treated organoids are viable; Inhibition of PI3K and Arp2/3 reduces protrusion rates.

(A-D) DIC images of organoids pharmacologically inhibited from Day 0. r=3. Scale = 50 µm. **(A'-D')** Epifluorescent images of associated organoids stained for viability (Calcein green, white = viable). Scale = 50 µm. **(A)** Vehicle (DMSO, 986 orgs). **(B)** 300 µM Arp2/3 inhibitor (CK-666, 933 orgs). **(C)** Vehicle + 4% PFA (DMSO, 928 orgs). **(D)** 300 µM Arp2/3 inhibitor + 4% PFA (CK-666, 1007 orgs). **(E)** Quantification of organoid viability (% viable, mean ± SD) upon CK-666 treatment. Vehicle (100 ± 0%), Vehicle + 4% PFA (0 ± 0%), 300 µM CK-666 (98.5 ± 0.5%), and 300 µM CK-666 + 4% PFA (0 ± 0%). r = 3. Two-tailed Mann Whitney test did not reach significance ($p > 0.05$), which means that viability was indistinguishable between vehicle and CK-666 treated conditions. **(F)** Time projection of cell migration and protrusions pre-and post-treatment with 50 µM PI3K inhibitor (LY-294002). Scale = 5 µm. Cell color codes time (blue, start; light gray, end). **(G)** Quantification of paired protrusion rate (#/hour) pre-and post-treatment with 50 µM PI3K inhibitor (LY-294002). N=10 cells, 3 orgs, r=3. Wilcoxon matched-pairs signed rank test, $p<0.01$. **(H)** Time projection of cell migration and protrusions pre-and post-treatment with 300 µM Arp2/3 inhibitor (CK-666). Scale = 5 µm. Cell color codes time (blue, start; light gray, end). **(I)** Quantification of paired protrusion rate (#/hour) pre-and post-treatment with 300 µM Arp2/3 inhibitor (CK-666). N=10 cells, 10 orgs, r=3. Wilcoxon matched-pairs signed rank test, $p<0.01$.

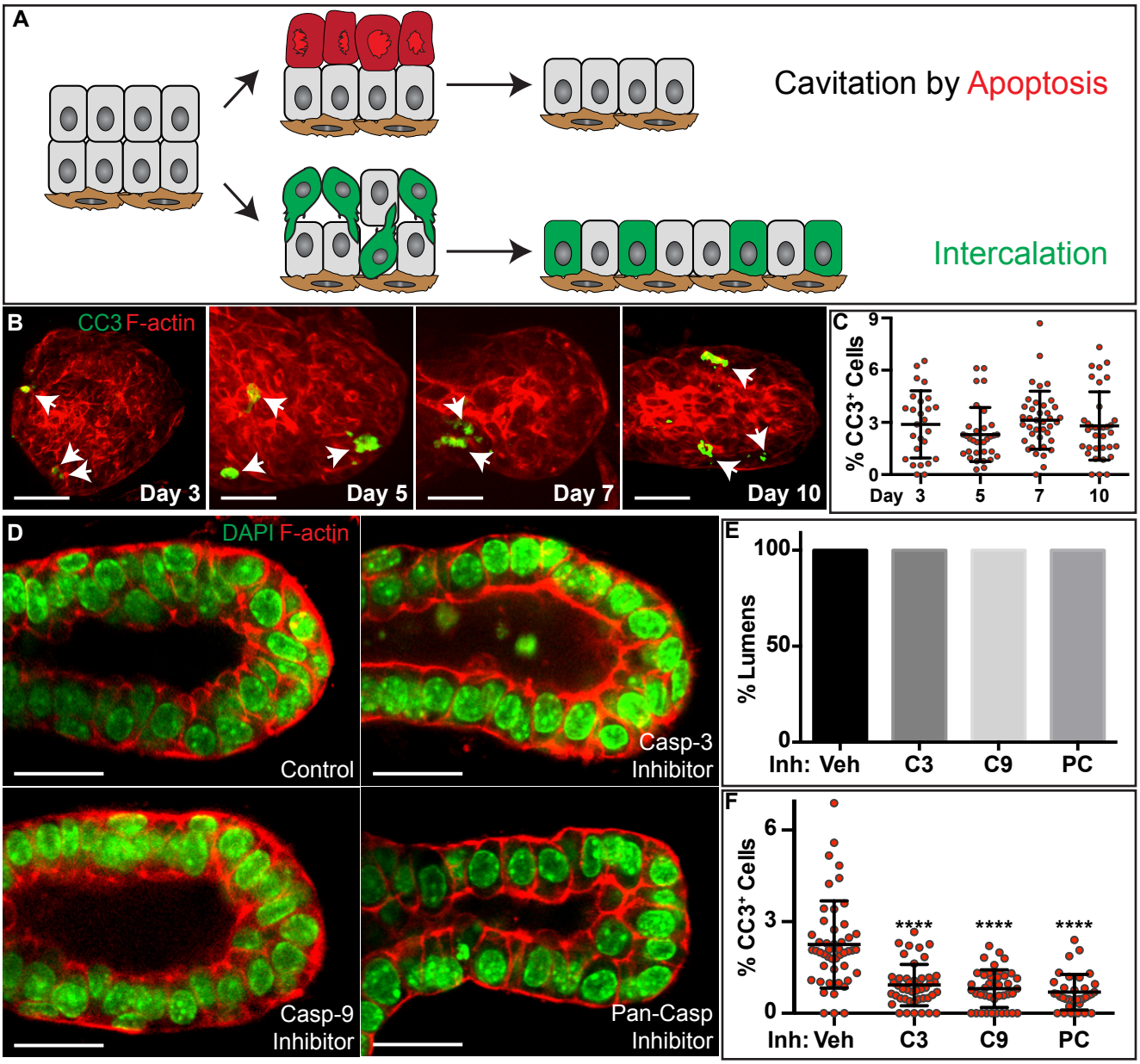

Figure S3 (Related to Figure 4) Bilayer formation does not require apoptosis.
(A) A model of bilayer formation by cavitation or intercalation. **(B)** 3D confocal projections of F-actin (phalloidin, red) and cleaved caspase-3 (CC3, green) from days 3, 5, 7, and 10 in culture. Scale = 20 μm. **(C)** Percent CC3+ cells from day 3 (26 organoids (orgs)), 5 (33 orgs), 7 (39 orgs), and 10 (34 orgs) (mean ± SD; r=4). Kruskal-Wallis test did not reach significance ($p > 0.05$), which means that CC3+ levels were not distinguishable over time. **(D)** 3D confocal projections of membranes (tdTomato, red) and nuclei (DAPI, green) of organoids treated with scrambled peptide control or caspase-3, caspase-9, or pan-caspase inhibitor, taken at 10 days. Scale = 20 μm. **(E)** Quantification of lumen formation at 10 days in organoids treated with scrambled peptide control (45 orgs), cleaved caspase-3 (33 orgs), cleaved caspase-9 (33 orgs), or pan caspase inhibitors (48 orgs). Lumen formation defined as branches containing a clear area between F-actin enriched apical membranes, with a maximum of 3 nuclei separating apical and basal tissue surfaces, to account for imaging plane effects. r=4. **(F)** Quantification of percentage of CC3+ cells in 3D confocal data. Even focal staining was counted as CC3+. CC3 levels were significantly reduced in each inhibitor condition (caspase-3 (0.93%, 35 orgs), caspase-9 (0.81%, 45 orgs), and pan caspase (0.69%, 40 orgs)), compared to vehicle (2.25%, 48 orgs) (mean ± SD; r=4). Kruskal-Wallis test, $p<0.0001$.

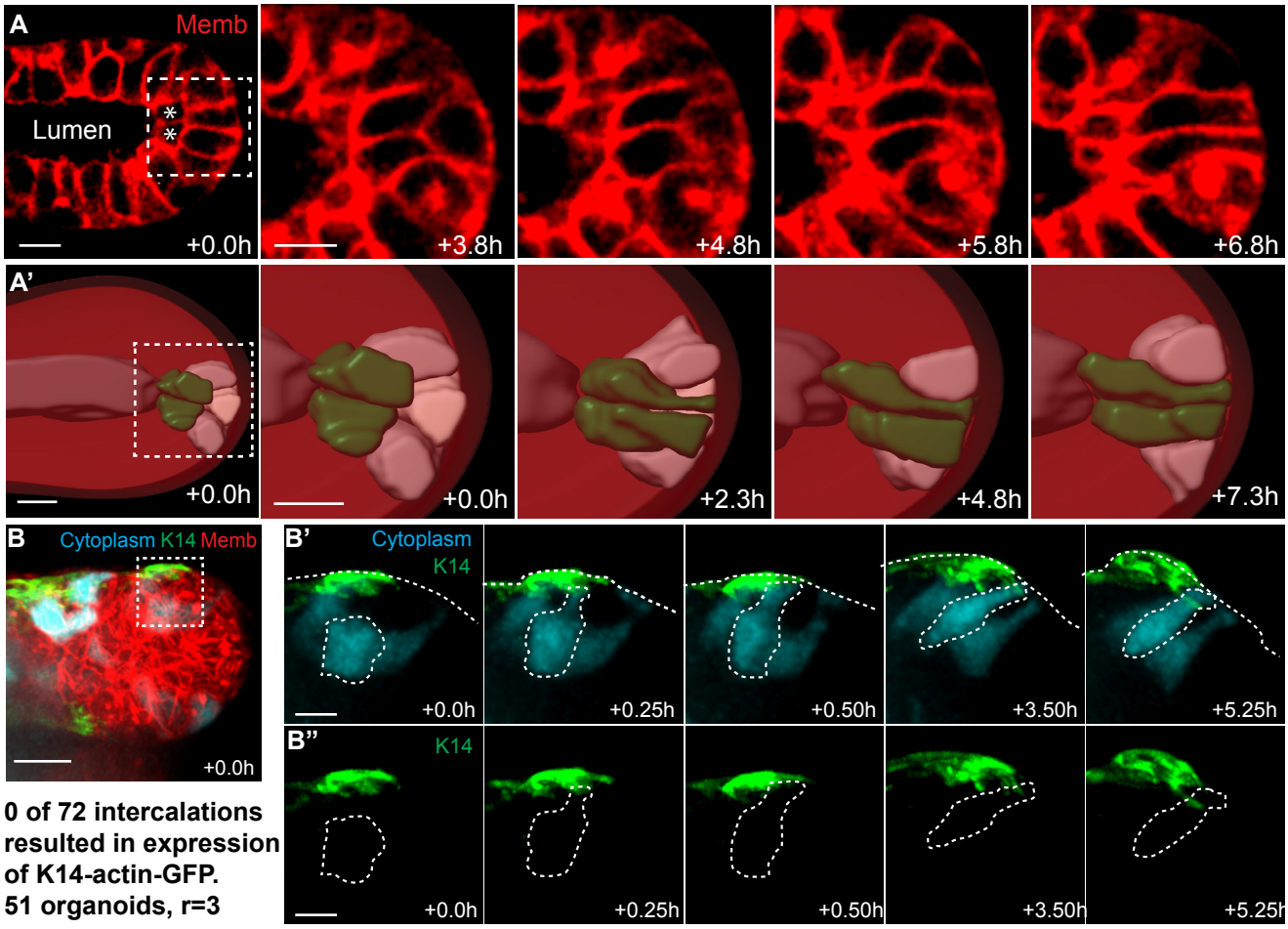

Figure S4 (Related to Figure 4) Luminal epithelial cells intercalate and establish a single luminal layer.
(A) A single plane from a 3D confocal time-lapse showing a branch that is polarized except for 4 cells in the front (white box). The two cells touching the lumen intercalate to contact the basal surface and establish a single luminal layer. **(A')** 3D surface rendering of the cell movements in (A) (Surfaces function; Imaris). Scale = 10 μm. (A) Scale = 20 μm. (A') Scale = 10 μm. **(B)** 3D confocal projections of mosaically labeled cytoplasm (CFP, cyan), myoepithelium (K14-actin-GFP, green), and membrane (tdTomato, red) during branch elongation. No intercalating cells were observed to upregulate expression of K14-actin-GFP, an indication of myoepithelial state, 0/72 cells, 51 organoids, r=3. Scale = 20 μm. **(B',B")** White box inset; 3D confocal projections of mosaically labeled cytoplasm (CFP, cyan) and myoepithelium (K14-actin-GFP, green) showing a representative luminal cell (white outline) intercalating without activating GFP expression. Scale = 10 μm.

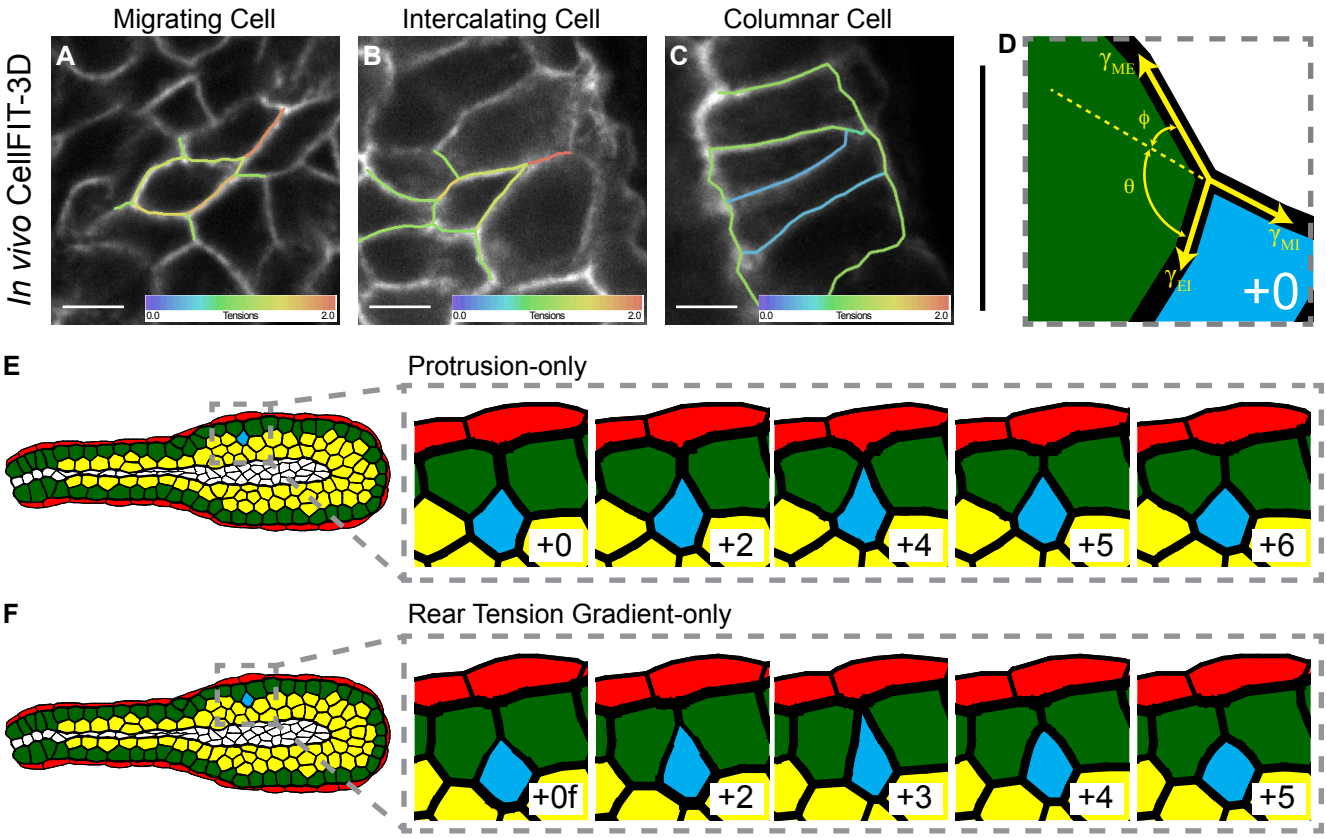

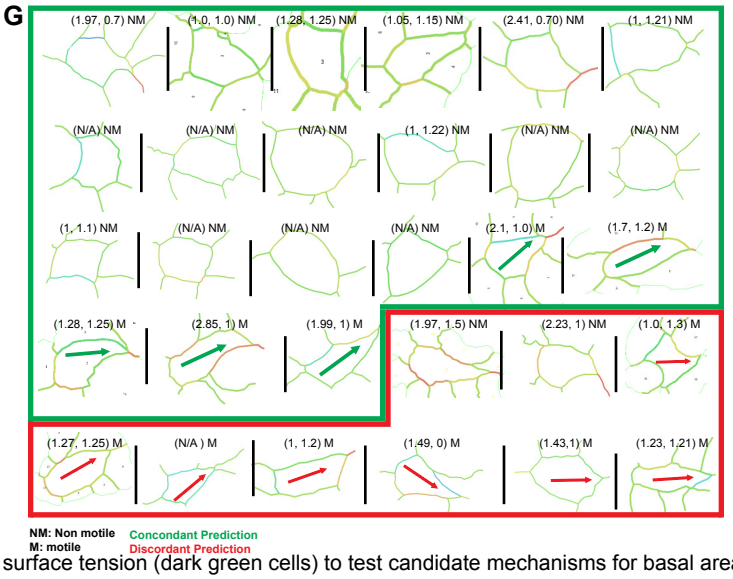

Figure S5 (Related to Figure 3, 6, & 7) In vivo CellFIT-3D Result; Epithelial cells predominantly cannot radially intercalate without boundary capture mechanism.

(A) CellFIT-3D was applied to confocal z-stacks of membrane labeled in vivo ducts and terminal end buds (tdTomato, green) to generate a mesh. Membranes were segmented using a watershed filter to reconstruct 3D cell shape. CellFIT-3D segments generated. Curvilinear triple junctions (where three cells meet) were reconstructed using vectors to define the relative angles between them. Apparently migratory cells were detected with a 'tear-drop' shape similar to that observed in 3D culture. CellFIT-3D analysis revealed high interfacial tension in the anterior protrusion and a gradient of tension increasing towards the posterior (not displayed in figure). Tension scale: low (violet) to high (red). **(B)** Apparently intercalating cells also exhibit high interfacial tension in the anterior protrusion and a gradient of tension increasing towards the posterior, similar to that observed in 3D culture (not displayed in figure). Tension scale: low (violet) to high (red). **(C)** Columnar epithelial cells display modestly higher anterior and posterior tensions, relative to lateral tensions. Tension scale: low (violet) to high (red). **(D)** A FEM was generated of a tissue with high basal surface tension (dark green cells) to test candidate mechanisms for basal area of an intercalating cell. A cell (blue) was captured at the basal surface through a combination of posterior tension and focal disruption of the high basal tissue tension. Principle tension components (γMI, γEI, γME, yellow arrows) acting at the two intercellular junctions. M, Matrix; I, Intercalating cell; E, Epithelial cell. The intercalated cell basal surface could then undergo 1 of 3 conditions – elongation, static, or shortening. $\delta = \gamma EI\cos\theta + \gamma ME\cos\phi$ **(E)** A FEM of a terminal end bud (TEB) testing intercalation success using only anterior protrusion or posterior tension gradient without the boundary capture mechanism described in Figure 5D". Interior cells could migrate and divide and a subset were randomly chosen to intercalate (blue), with random protrusion and tension gradient strengths, directed towards the basal most luminal cell layer (green cells). The model also included high basal tension and in-plane stress applied towards the organoid center-line (hoop stress), to model the function of the contractile myoepithelium (red). The lumen does not affect cellular tensions. This mechanism resulted in few intercalations and did not efficiently elongate the tissue. **(F)** Posterior tension gradient-only intercalation without the boundary capture mechanism described in Figure 5D". This mechanism resulted in few intercalations and did not efficiently elongate the tissue. **(G)** CellFIT-3D was used to define the relative strength of anterior protrusions and posterior tension gradients in 30 cells from elongating organoids. The criteria defined in Figure 3K were used to predict whether the cell would migrate. Blinded predictions correctly identified the migratory outcome in 21/30 cells. Two-tailed Fischer's exact test for contingency tables, $p = 0.0837$. Predictions were highly accurate in identifying non-migratory cells (16/18) but similar to chance in identifying migratory cells (5/12), suggesting that the tension relationships represented in the cell shape are necessary but not sufficient for migration.

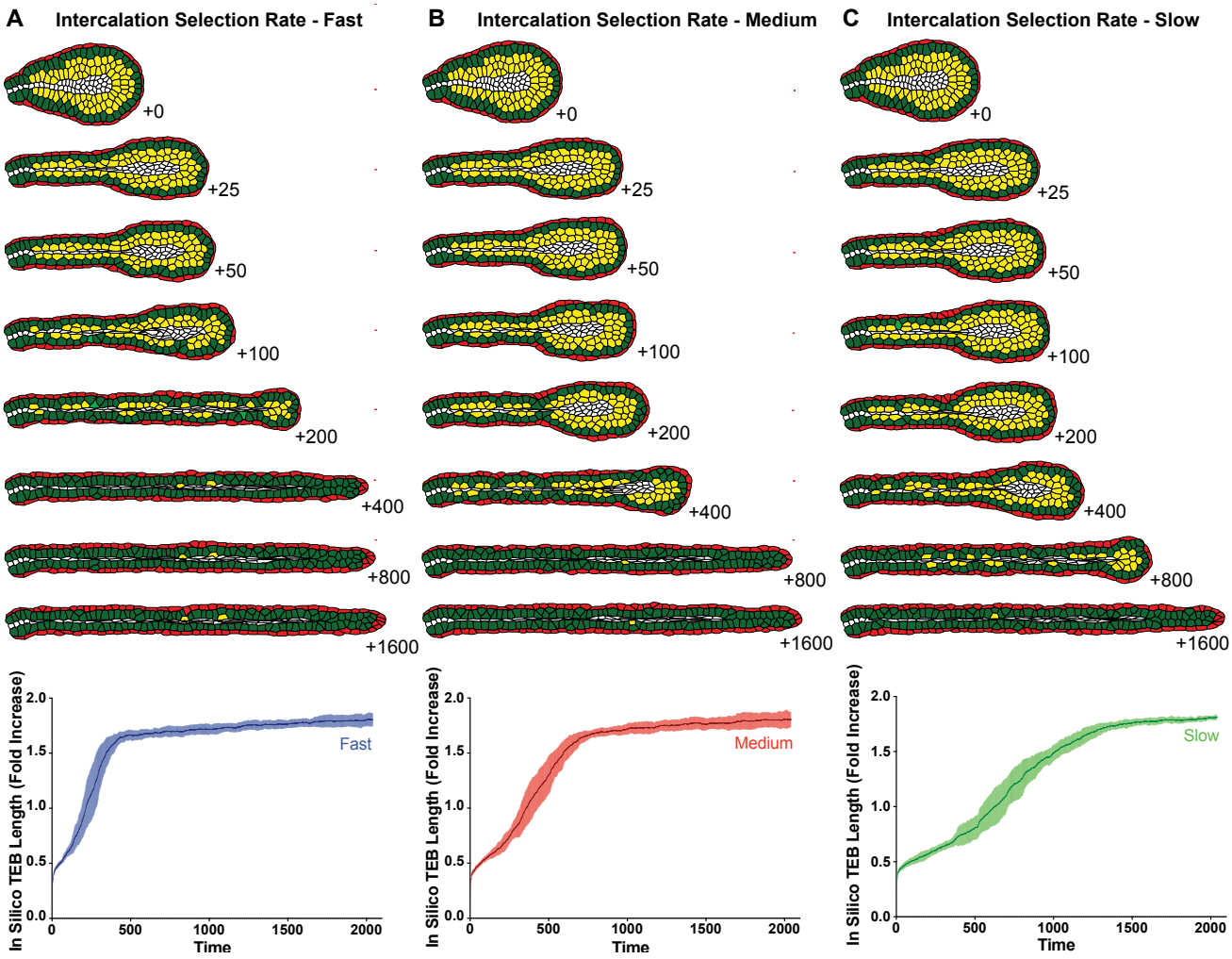

Figure S6 (Related to Figure 7) Tube elongation rate is dependent on intercalation selection rate.
(A-C) A FEM of a terminal end bud (TEB), similar to Figure 7B, testing the influence of intercalation selection rate on tube elongation rate. Interior cells (yellow) were randomly chosen at a selection of **(A)** 2x (termed, “Fast”), **(B)** x (termed, “Medium), and **(C)** 0.5x (termed, ”Slow) to intercalate with random protrusions and tension gradient strengths, directed towards the basal most luminal cell layer (green cells). High basal tension and in-plane stress applied towards the TEB center-line (hoop stress) was applied to model the function of the contractile myoepithelium (red). The hoop stress marched along the TEB as it transitioned to a bilayer architecture. Time is in dimensional units (see STAR Methods). The TEB length fold increase is reported in the plot. n=10 simulations per condition.